tunnel effect is essential for these reactions.

Vibrational anharmonicity is not considered in the present work.

The threshold energies from three-dimensional quantum scattering calculations[66] on reaction 1 were previously found to be less than the potential barrier height or the vibrationally adiabatic barrier height.[56] It was found that model BC fitted the data well. However model BC did not agree with one- and two-dimensional quantum scattering calculations. Here we find that model BC works well for reactions 3, 5, and 6.

Two major weaknesses of the present approach are the use of a simple one-dimensional tunneling factor and the use of one of three simple expressions for the bending partition function. In ref 56 it was found that replacing an Eckart barrier by a parabolic barrier decreased log A by 0.1 and E_e by 1.8 kJ mol^{-1}. Allowing for excited bending states in model Q made similar differences. Thus uncertainties introduced by the model are comparable to those introduced by the data.

Another weakness is the fact that a quantum chemical bending frequency was used to help in choosing the best model for a particular reaction. For some reactions no ab initio bending frequency may be available and it might be necessary to use a semiempirical frequency. It has been shown that reasonable results can be obtained even when the choice of model is not clear cut.

It would be interesting to apply the present method to other reactions, especially those with extensive experimental data and accurate quantum chemical calculations. The method can also be improved. Alternate treatments of the vibrational degrees of freedom are possible. The present results show that the symmetric stretching mode can be treated as unexcited. The internuclear distances needed to calculate the moments of inertia could be estimated with reasonable accuracy by semiempirical methods.[46,53] The only remaining quantity needed to calculate log A in eq 16 and 18 is the bending frequency. The bending frequency could be treated as the variable parameter, instead of log A. It would then be possible to use exact expressions for the bending partition function, instead of the present approximations.[67] Such a method would provide more specific information about the transition state from curved Arrhenius plots.

Acknowledgment. The authors thank the Natural Sciences and Engineering Research Council of Canada for a grant in support of this work, D. G. Truhlar for a preprint of ref 17, and J. A. Coxon, K. Darvesh and F. Grein for valuable discussions.

Registry No. H_2, 1333-74-0.

(66) Schatz, G. C.; Kuppermann, A. *J. Chem. Phys.* **1976**, *65*, 4668.

(67) Furue, H.; Pacey, P. D., to be published.

Thermal and Photochemical Reactions of Sulfhydryl Radicals. Implications for Colloid Photocorrosion

G. Mills, K. H. Schmidt, M. S. Matheson, and D. Meisel*

Chemistry Division, Argonne National Laboratory, Argonne, Illinois 60439 *(Received: July 25, 1986; In Final Form: October 29, 1986)*

Several thermal and photochemical reactions of sulfhydryl radicals, either in their monomeric ($S^{\bullet-}/HS^{\bullet}$) or dimeric ($H_2S_2^{\bullet-}$) form, have been studied by using the pulse radiolysis technique. The dimer form is shown to react with O_2 and methylviologen (MV^{2+}). The monomer reacts with O_2 to produce a transient addition product, $SO_2^{\bullet-}$, which further proceeds to give superoxide radicals. The dimer reacts slower with O_2 by electron transfer. The reaction of $S^{\bullet-}/SH^{\bullet}$ with MV^{2+} yields several addition products which strongly absorb at $\lambda_{max} = 485$ nm. These are partially converted to $MV^{\bullet+}$, either through a unimolecular process or by reaction with another MV^{2+} molecule. Implications of these observations for the photocorrosion of semiconductor colloidal sulfides are discussed. In particular, the possibility of reduction processes by surface-adsorbed sulfhydryl radicals, produced by hole trapping at the colloid surface, is considered.

Photochemistry at semiconductor sulfide surfaces either in a photoelectrochemical cell or in colloidal suspensions is a subject of intense activity in recent years.[1] Following photoexcitation of the sulfide material, electron–hole pairs are formed which may either recombine or be scavenged by electron donors or acceptors. A common electron donor which may transfer electrons to the photocreated hole is the sulfide ion itself, inevitably present in such systems either at the material surface or sometimes in the bulk electrolyte. In the absence of excess sulfide ions (or other electron donors), the hole may eventually lead to anodic corrosion of the material and formation of elemental sulfur and/or higher oxysulfur oxidation products. On the other hand, in the presence of excess sulfide the photocorrosion process is efficiently inhibited by electron injection from the reservoir of bulk sulfide ions to scavenge the holes, provided electrons are scavenged as well. In both cases of hole scavenging, sulfide radicals may be produced and further react with various components of the system, either in the bulk of the solution or at the semiconductor/electrolyte interface. Indeed, formation of sulfhydryl radicals and their subsequent electron transfer to oxygen have been recently invoked to rationalize the effect of oxygen on the photocorrosion of CdS colloids.[2,3] In this context, we undertook the present study on the reactivity of sulfhydryl radicals. In particular, we focused our attention on the reactions of these radicals with two of the most commonly utilized electron acceptors, O_2 and methylviologen (MV^{2+}).

Oxidation of H_2S in aqueous solutions upon irradiation with ionizing radiation has been studied previously.[4] From these results, it was concluded that all the primary radicals in irradiated aqueous solutions of H_2S (i.e., e_{aq}^-, $OH^{\bullet}$, $H^{\bullet}$) are converted to

(1) An extensive list of references can be found in: (a) Hodes, G.; Grätzel, M. *Nouv. J. Chim.* **1984**, *8*, 509. (b) Bard, A. J. *J. Photochem.* **1979**, *10*, 59. (c) Ramsden, J. J.; Grätzel, M. *J. Chem. Soc., Faraday Trans. 1* **1984**, *80*, 919.

(2) (a) Henglein, A. *Ber. Bunsenges. Phys. Chem.* **1982**, *86*, 301. (b) Henglein, A.; Gutierrez, M. *Ber. Bunsenges. Phys. Chem.* **1983**, *87*, 852.

(3) Meissner, D.; Memming, R.; Shuben, L.; Yesodharan, S.; Grätzel, M. *Ber. Bunsenges. Phys. Chem.* **1985**, *89*, 121.

(4) Karmann, W.; Meissner, G.; Henglein, A. *Z. Naturforsch.* **1967**, *22B*, 273.

0022-3654/87/2091-1590$01.50/0

TABLE I: Kinetic Parameters for the Formation and Decay of $HS^{\bullet}/H_2S_2^{\bullet-}$ Radicals[a]

reaction	k, M^{-1} s^{-1}
$e_{aq}^- + H_2S \rightarrow H^{\bullet} + HS^-$	1.1×10^{10} [b]
$H^{\bullet} + H_2S \rightarrow H_2 + HS^{\bullet}$	9.0×10^{9} [b]
$OH^{\bullet} + H_2S \rightarrow H_2O + HS^{\bullet}$	1.1×10^{10} [b]
$OH^{\bullet} + HS^- \rightarrow HSOH^{\bullet-}$	5.4×10^{9} [b]
$HS^{\bullet} + HS^- \rightarrow H_2S_2^{\bullet-}$	5.4×10^{9}
$H_2S_2^{\bullet-} \rightarrow HS + HS^-$	5.3×10^{5}
$2H_2S_2^{\bullet-} + H_2S_2 + 2HS^-$	9.5×10^{8}
$2HS^{\bullet} \rightarrow H_2S_2$	6.5×10^{9}
$HS^{\bullet} + H_2S_2^{\bullet-} \rightarrow H_2S_2 + HS^-$	9.0×10^{9}
$HSOH^{\bullet-} + HS^- \rightarrow H_2S_2^- + OH^-$	2.0×10^{9} [c]
$HSOH^{\bullet-} + H_2S \rightarrow H_2S_2^{\bullet-} + H_2O$	3.0×10^{9} [c]
$O_2 + HS^{\bullet} \rightarrow SO_2^- + H^+$	7.5×10^{9}
$O_2 + H_2S_2^{\bullet-} \rightarrow O_2^- + H_2S_2$	4.0×10^{8}

[a] All results were obtained at pH 7.0 ± 0.1. [b] Reference 4. [c] Estimated; observed rate is insensitive to these rate constants.

$HS^{\bullet}$ (or $S^{\bullet-}$) radicals. These, however, further complex with HS^- to form the easily detectable (λ_{max} = 380 nm, $\epsilon_{380} \sim 10^4$ M^{-1} cm^{-1}) complex $H_2S_2^{\bullet-}$ radical (eq 1). The association constant for the

$$HS^{\bullet} + HS^- \rightleftarrows H_2S_2^{\bullet-} \quad (1)$$

latter had been determined to be $K_1 = 2.5 \times 10^4$ M^{-1}.[4] The reactive radical in such a system might, therefore, be either the monomeric or the complex radical or both. Both radicals are shown in this report to react with O_2 and MV^{2+}.

Another point addressed in this study is the fate of the $H_2S_2^{\bullet-}$ radical upon excitation to its first excited state. As might be expected from theoretical considerations[5] and similar to the situation with other three-electron-bonded radicals (e.g., dihalide radical anions),[6] the first excited state is shown to be a repulsive state dissociating back to give its parent components.

Experimental Section

Deaerated water was used to prepare H_2S (Matheson, C.P.) saturated stock solutions (assumed 0.113 M) a few hours before irradiation. These were mixed with solutions containing the other components to yield the final desired solutions immediately before irradiation using the syringes technique. Water was triply distilled, and all chemicals were of highest purity commercially available. Unless otherwise stated, all experiments were performed at pH 7 in the presence of 2 mM phosphate buffer. In the following, H_2S concentrations are given as total sulfide concentration. At pH 7, 50% will be in the form of HS^-.

Conventional pulse radiolysis has been used to produce the radicals (1–4-ns pulse width, 0.2–1 krad/pulse). Spectrophotometric detection using a monochromator/photomultiplier combination was used to follow kinetics or to record transient spectra. For radicals absorbing above 320 nm, the streak camera technique[7a] was utilized to record spectra. The pulse radiolysis/laser flash photolysis setup has been previously described.[7b] Data were collected on an LSI 11/23 minicomputer and were later transferred to a VAX 11/80 computer for processing and analysis.

Results and Discussion

$H_2S_2^{\bullet-}$ and Higher Complexed Radicals. Results similar to those previously reported[4] on the oxidation of H_2S in irradiated aqueous solution have been observed in the present study. More detailed analysis was, however, necessary for further studies of the reactions of the radicals formed with other scavengers. Results are included in Table I. The absorption at 380 nm increases with increased $[H_2S]$ at pH 7. However, at high H_2S concentrations, this absorption does not level off. Instead, a slow increase is continuously observed. This increase in the absorption is attributed, as previously suggested, to higher polysulfide radicals such as $H_4S_3^{\bullet-}$.[4] The equilibrium constant for reaction 1 was determined at $[H_2S] \leq 1 \times 10^{-3}$ M (pH 7) from plots of 1/OD vs. $1/[HS^-]$, as shown in Figure 1. The intercept in this figure is equal to $1/OD_0$, where OD_0 is the absorbance at complete conversion of the radicals to $H_2S_2^{\bullet-}$. From the intercept we obtain $\epsilon_{380} = 7000$ M^{-1} cm^{-1}. The equilibrium constant presently obtained is somewhat smaller (Table I) than previously reported,[4] probably due to neglect of the higher complex radicals. The latter seem to have a higher extinction coefficient than $H_2S_2^{\bullet-}$ at 380 nm. Another complication in this system may arise from the various pK_a's of the radicals involved. None of these are known, yet the pK_a of the $HS^{\bullet}$ radical is most probably lower than that of H_2S (pK_a = 7). In fact, as will be shown in the section dealing with MV^{2+} reactions, $S^{\bullet-}$ is the major reactive form rather than $HS^{\bullet}$ at pH 7.

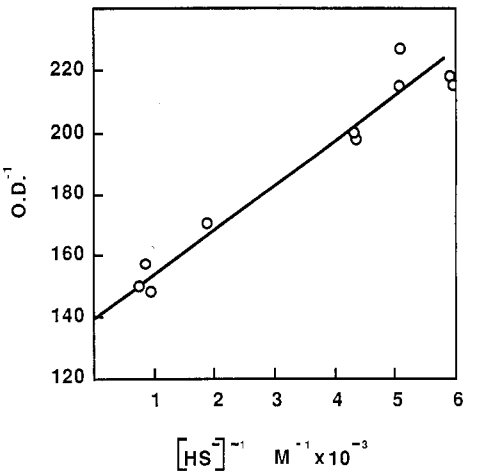

Figure 1. Determination of the equilibrium constant for $HS^{\bullet} + HS^- \rightleftarrows H_2S_2^{\bullet-}$. λ = 380 nm.

Three decay modes of $H_2S_2^{\bullet-}$ were assumed (eq 2a–2c), and a nonlinear least-squares procedure was used to estimate the individual rate constants[8] from the observed second-order decay rate constant at various H_2S concentrations. Since the decay

$$2H_2S_2^{\bullet-} \xrightarrow{H^+} H_2S_2 + 2H_2S \quad (2a)$$

$$H_2S_2^{\bullet-} + HS^{\bullet} \rightarrow H_2S_2 + HS^- \quad (2b)$$

$$2HS^{\bullet} \rightarrow H_2S_2 \quad (2c)$$

rate constant levels off at high H_2S concentrations, it was assumed that the higher polysulfide complex radicals decay with the same rate constants as the $H_2S_2^{\bullet-}$ radical. Individual kinetic decay traces were then simulated by using the values obtained from least-squares procedure (given in Table I) and were found to closely follow the experimentally obtained results. It should also be noted that the decay kinetics of the absorption at 380 nm always followed a pure second-order, equal concentration rate law, in the absence of any reactive additive. However, upon addition of such scavengers the decay followed an exponential rate law. The kinetic parameters given in Table I were fixed in the calculation of rate constants with oxygen described below.

Photochemistry of $H_2S_2^{\bullet-}$ Radicals. Excitation of disulfide radical cations, including $H_2S_2H_2^{\bullet+}$, has been attributed to a $\sigma \rightarrow \sigma^*$ transition.[5,9] For $H_2S_2H_2^{\bullet+}$, ab initio molecular orbital calculations, however, indicate considerable nonbonding character in the highest fully occupied molecular orbital.[10] The isoelectronic $H_2S_2^{\bullet-}$ radical is expected to have a similar transition, and both radicals have practically identical transition energies. In the gas phase vertical excitation into this σ^* state is expected to lead to dissociation along the S–S three-electron bond. In a polar solvent, however, the possibility of photodetachment to yield solvated

(5) Asmus, K. D. *Acc. Chem. Res.* **1979**, *12*, 436.
(6) Nagarajan, V.; Fessenden, R. W. *J. Phys. Chem.* **1985**, *89*, 2330.
(7) (a) Schmidt, K. H.; Gordon, S.; Mulac, W. A. *Rev. Sci. Instrum.* **1976**, *47*, 356. (b) Bromberg, A.; Schmidt, K. H.; Meisel, D. *J. Am. Chem. Soc.* **1985**, *107*, 83.
(8) Capellos, C.; Bielski, B. H. J. *Kinetic Systems*; Wiley-Interscience: New York, 1972; p 65.
(9) Chaudhri, S. A.; Asmus, K. D. *Angew. Chem., Int. Ed. Engl.* **1981**, *20*, 672.
(10) Clark, T. *J. Comput. Chem.* **1981**, *2*, 261.

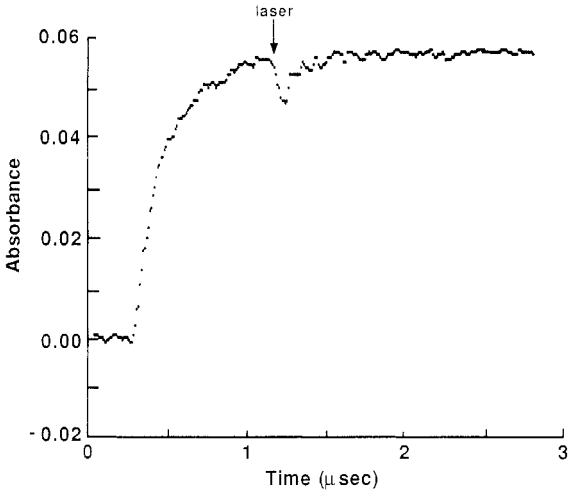

Figure 2. Photodissociation of $H_2S_2^{\bullet-}$. Solution contains 4.5×10^{-3} H_2S, 2 mM phosphate buffer (pH 7, Ar saturated). λ_{exc} = 347 nm, followed at 380 nm.

electrons has to be considered. The situation with this radical is thus similar to that of dihalide radical ions. For the latter radicals excitation in aqueous solutions leads to photodissociation.[6]

Excitation of $H_2S_2^{\bullet-}$ (λ_{exc} = 347 nm) at pH 7 results in partial bleaching of its absorption at 380 nm (Figure 2) followed by recovery. Upon excitation of $H_2S_2^{\bullet-}$ at pH 9.0 (1.1×10^{-3} H_2S, 2 mM borate buffer) similar bleaching is observed when the radical is followed at 380 nm. However, no formation of absorption, which might be attributed to e_{aq}^-, could be observed at 600 nm, following the laser pulse. Since $\epsilon_{600}(e_{aq}^-) > \epsilon_{380}(H_2S_2^{\bullet-})$ and since the half-life of e_{aq}^- in this solution is ca. 2 μs, we can exclude ($\Phi < 0.05$) the possibility of photodetachment of electrons upon excitation of $H_2S_2^{\bullet-}$ to its first excited state. The rate of recovery of the absorption at 380 nm depends linearly on [H_2S] at pH 9 and yields $k_1 = 2.6 \times 10^9$ M^{-1} s^{-1}, which is somewhat slower than the observation from pulse radiolysis at pH 7. The quantum yield for the bleaching, calculated assuming that the photoproducts do not absorb at the wavelength of detection, is $\Phi = 0.4 \pm 0.1$, significantly higher than the quantum yield for photodissociation of the dihalide radical ions.[6]

Reactions with Oxygen. Addition of oxygen to the solution accelerates the rate of decay of absorption of $H_2S_2^{\bullet-}$ and changes it to an exponential decay. The decay rate depends, under these conditions, on both oxygen and H_2S concentrations. As can be seen in Figure 3, the observed rate constant increases on increasing [O_2] and decreases on increasing [H_2S]. At high [H_2S] the observed rate constant levels off and becomes independent of [H_2S]. This dependence on concentration indicates that both $H_2S_2^{\bullet-}$ and $HS^\bullet$ radicals react with oxygen, the latter with a higher rate constant.

$$H_2S_2^{\bullet-} + O_2 \rightarrow P_1 \quad (3)$$

$$HS^\bullet + O_2 \rightarrow P_2 \quad (4)$$

Under conditions where equilibrium 1 is rapidly achieved as compared to the decay rate, the observed rate constant can be expressed by

$$k_{obsd} = \frac{k_4 + k_3K_1[HS^-]}{1 + K_1[HS^-]}[O_2] \quad (5)$$

Under such conditions (high [H_2S] and relatively low [O_2]) the observed rate constant indeed increases linearly with [O_2]. At the plateau level of Figure 3, the decay is primarily through reaction 3, and from the linear dependence on [O_2] in this region we obtain $k_3 = 4.0 \times 10^8$ M^{-1} s^{-1}. At low [H_2S], the rate of approach to equilibrium 1 is comparable to the decay rate and eq 5 no longer holds. For results under these conditions, we simulated the formation and decay profile of $H_2S_2^{\bullet-}$ absorption to obtain $k_4 = (7.5 \pm 1.0) \times 10^9$ M^{-1} s^{-1}. The sensitivity of such

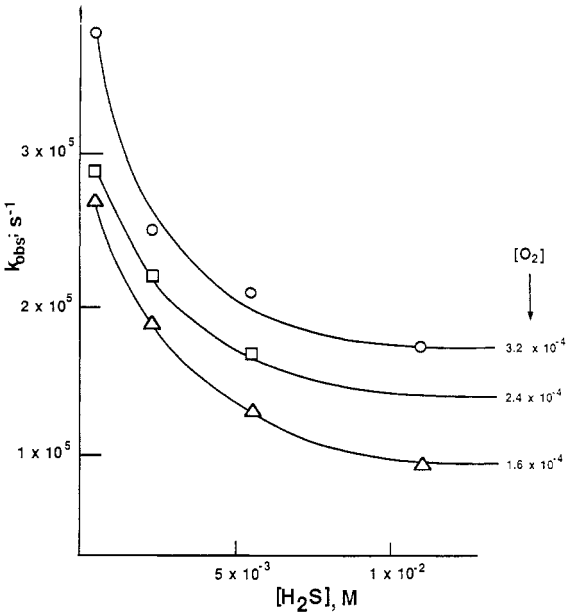

Figure 3. Dependence of the observed pseudo-first-order decay rate of $H_2S_2^{\bullet-}$ on H_2S and O_2 concentrations: (a) [O_2] = 1.6×10^{-4} M; (b) 2.4×10^{-4} M; (c) 3.2×10^{-4} M.

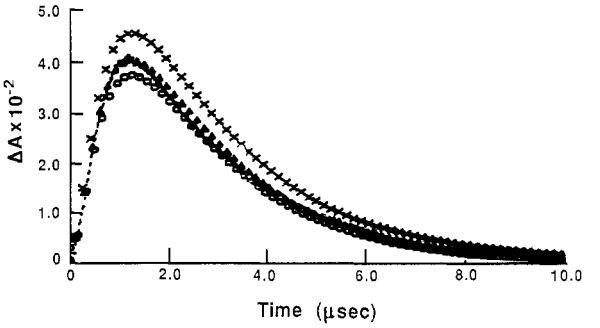

Figure 4. Simulation of the decay of $H_2S_2^{\bullet-}$ in the presence of oxygen. Middle curve is best fit to experimental results using the parameters in Table I ([O_2] = 3.2×10^{-4} M; [HS^-] = 4.5×10^{-4} M). Upper and lower curves are calculated using k_4 smaller or larger, respectively, by 15%.

simulations to changes in k_4 is shown in Figure 4. The strongest effect of changes in k_4 in the simulation is on the amplitude of the $H_2S_2^{\bullet-}$ absorbance. The accuracy therefore of k_4 determined by this method is limited by the accuracy of the determination of the extinction coefficient at the wavelength of observation.

In an effort to identify the products of reactions 3 and 4, we recorded the spectra of these products in the 250–350-nm region. The spectrum of $O_2^{\bullet-}$ as well as the spectrum of $H_2S_2^{\bullet-}$ in that region are shown in Figure 5, a and b, respectively. When oxygen is added to the same solution, producing spectrum 5b, a new absorption band is observed (Figure 5c) at the end of the formation of $H_2S_2^{\bullet-}$ radicals when followed at 380 nm (i.e., ~0.5 μs after the pulse). Under the conditions of Figure 5c, oxygen interferes with the establishment of equilibrium 1 and only ca. 70% of the total yield of the radicals produced $H_2S_2^{\bullet-}$. The remainder react through reaction 4. Since the spectrum obtained at this time cannot be reconstructed by any linear combination of the spectra of $O_2^{\bullet-}$ and $H_2S_2^{\bullet-}$, we conclude that the immediate product of reaction 4 is not $O_2^{\bullet-}$. A possible candidate for such a product is an $HSO_2^\bullet/SO_2^{\bullet-}$ species. The spectrum obtained at the end of the decay of $H_2S_2^{\bullet-}$ is shown in Figure 5d. While spectrum 5d still differs from that of O_2^-, the difference is less pronounced. At this time, most of $H_2S_2^{\bullet-}$ has already reacted through reaction 3 and the spectrum now is probably a composite of the two products. The product of reaction 3 therefore seems to be $O_2^{\bullet-}$. Attempts to obtain exclusively the spectrum of the product of reaction 3 at high H_2S concentrations were defeated due to strong absorption by HS^- in the UV region and rapid precipitation of colloidal sulfur at these high [H_2S] in the presence of oxygen.

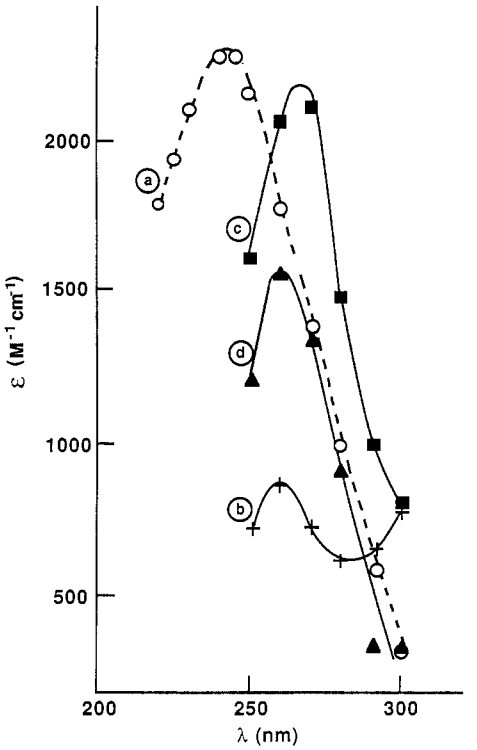

Figure 5. Spectra of the products of the reaction of $H_2S_2^{\bullet-}/HS^{\bullet}$ with O_2: (a) spectrum of $O_2^{\bullet-}$ (10^{-2} M $NaHCO_2$, 8×10^{-4} M O_2); (b) spectrum of $H_2S_2^{\bullet-}/HS^{\bullet}$ (4.5×10^{-4} M H_2S, 2.0×10^{-2} M N_2O); (c) spectrum as in (b) containing 3.2×10^{-4} M O_2 at $t = 0.5$ μs after the pulse; (d) spectrum as in (c) at $t = 5.0$ μs after the pulse. All solutions buffered at pH 6.90; spectra b–d are corrected for the small bleaching in the absorption of the H_2S/HS^- system.

Two further points may be made regarding the oxygen adduct formed in reaction 4. The spectrum of $SO_2^{\bullet-}$ radicals has been previously reported to peak at 365 nm.[11] The presently observed spectrum is clearly different from the one previously observed. This, however, is to be expected since the adduct radical presently observed is envisioned to be a peroxy radical. Furthermore, as can be seen in Figure 5, the absorption at 270 nm decays on the same time scale that reactions 3 and 4 are proceeding. This leads us to conclude that the adduct radical is an intermediate which decays to produce another radical, presumably $O_2^{\bullet-}$.

Reactions with MV^{2+}. Since MV^{2+} is often used as an electron acceptor for photogenerated electrons in semiconductor sulfides, we investigated the possible reactions between MV^{2+} and the sulfhydryl radicals. It is now well established that MV^{2+} forms ion pairs or charge-transfer complexes with a variety of anions in aqueous solutions.[12] Indeed, sulfide–MV^{2+} ion pairs have been observed to exhibit a charge-transfer absorption band at 410 nm.[12d] However, under the experimental conditions of the present study, the absorption spectra of H_2S/MV^{2+} mixtures are identical with the sum of the spectra of the separate components. We therefore discuss the present results in terms of the separate ions. Nevertheless, it is realized here that ion pairs, in particular 1:1 pairs of MV^{2+} and HS^-, may exist in our systems.

The possibility of a reaction between $MV^{\bullet+}$ and H_2S/HS^- was investigated through preferential production of $MV^{\bullet+}$ (1 M 2-propanol, 10^{-2} M $MV^{\bullet 2+}$, $[H_2S] = (0.1–1.0) \times 10^{-3}$ M, pH 7). Under these conditions, more than 90% of the primary radicals produced by the radiolysis of water are converted to $MV^{\bullet+}$ within a few microseconds following the pulse.[13] No decay of $MV^{\bullet+}$ could be observed in this H_2S concentration range, thus excluding any reaction of $MV^{\bullet+}$ with the H_2S system. We further noticed that the blue color of $MV^{\bullet+}$ could be observed by eye many seconds after the pulse.

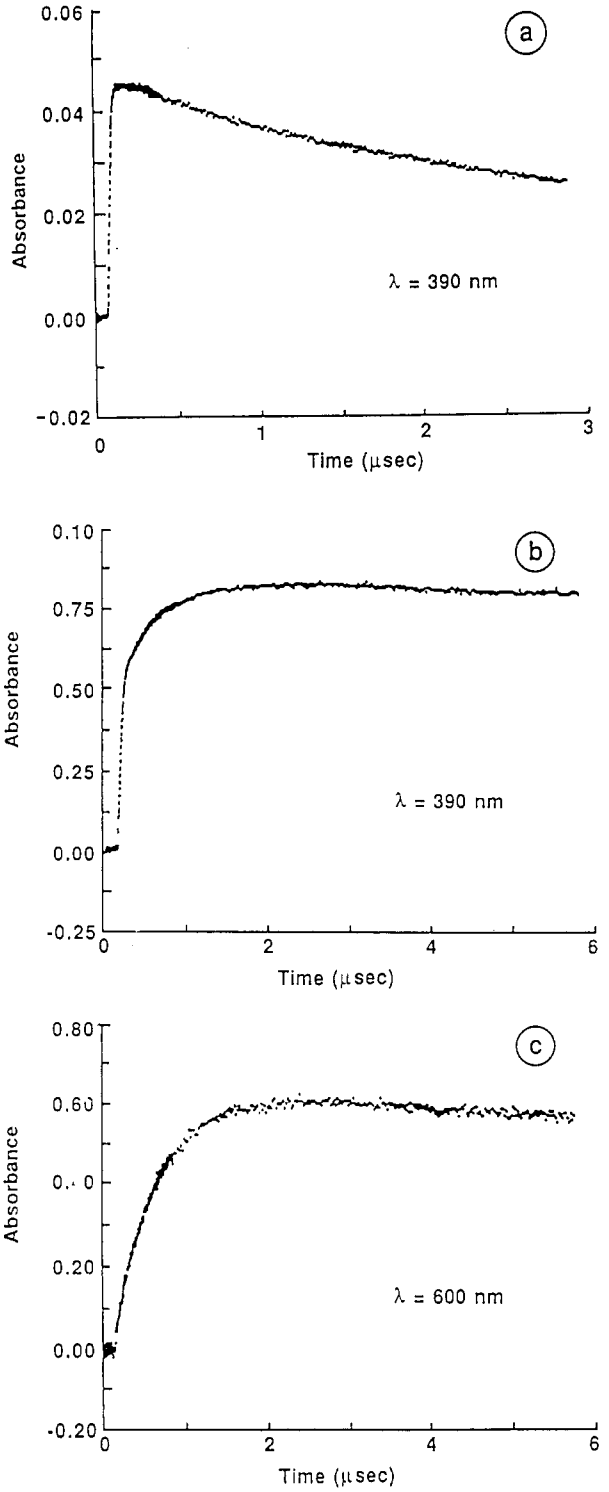

Figure 6. Formation of $MV^{\bullet+}$ by the reaction of sulfhydryl radicals in solution containing 1.1×10^{-3} M H_2S at pH 7 saturated with N_2O: (a) no MV^{2+}; (b, c) 3.6×10^{-4} M MV^{2+}. Absorption followed at the indicated wavelengths.

(11) Hayon, E.; Treinin, A.; Wilf, J. *J. Am. Chem. Soc.* **1972**, *94*, 47.
(12) (a) Ebbesen, T. W.; Ferraudi, G. *J. Phys. Chem.* **1983**, *87*, 3717. (b) Ebbesen, T. W.; Manring, L. G.; Peters, K. S. *J. Am. Chem. Soc.* **1984**, *106*, 7400. (c) Ebbesen, T. W.; Levey, G.; Patterson, K. K. *Nature (London)* **1982**, *298*, 545. (d) Kuczynski, J. P.; Milosavljevic, B. H.; Lappin, A. G.; Thomas, J. K. *Chem. Phys. Lett.* **1984**, *104*, 149. (e) White, B. G. *Trans. Faraday Soc.* **1969**, *65*, 200. (f) Poulos, A. T.; Kelley, C. K.; Simone, R. *J. Phys. Chem.* **1981**, *85*, 823. (g) Sullivan, B. P.; Dressick, W. J.; Meyer, T. J. *J. Phys. Chem.* **1982**, *86*, 1473. (h) Harriman, A.; Porter, G.; Wilowska, A. *J. Chem. Soc., Faraday Trans. 2* **1984**, *80*, 191. (i) Barnett, J. R.; Hopkins, A. S.; Ledwith, A. *J. Chem. Soc., Perkin Trans. 2* **1984**, *80*. (j) Hoffman, M. Z.; Prasad, D. R.; Jones, G.; Malba, V. *J. Am. Chem. Soc.* **1983**, *105*, 6360. (k) Prasad, D. R.; Hoffman, M. Z. *J. Phys. Chem.* **1984**, *88*, 5660.

(13) Meisel, D.; Mulac, W. A.; Matheson, M. S. *J. Phys. Chem.* **1981**, *85*, 179.

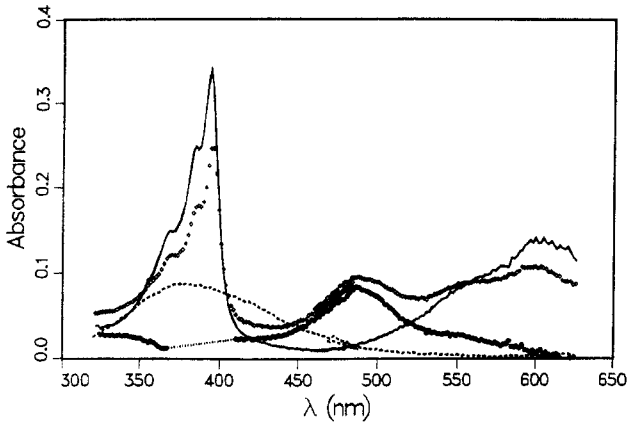

Figure 7. Spectrum of $H_2S_2^{\bullet-}$ (dashed), obtained in 10^{-3} M H_2S solution, N_2O saturated; spectrum of $MV^{\bullet+}$ (solid), obtained in 10^{-3} M MV^{2+} solution containing 0.1 M 2-propanol, Ar saturated (dose is half of that used for the other spectra); spectrum obtained in 10^{-3} M H_2S and 10^{-3} M MV^{2+} Ar-saturated solution (open squares); previous spectrum after subtraction of the spectrum of $MV^{\bullet+}$ (solid circles). Dotted line indicates the region where contribution from MV^+ alone is assumed. Spectra were taken at the end of the formation process using the streak camera technique.

Upon addition of MV^{2+} to H_2S in which $H_2S_2^{\bullet-}/HS^{\bullet}$ radicals are preferentially formed by the primary radicals ($[H_2S]$ = $(0.11-2.25) \times 10^{-3}$ M, N_2O saturated, pH 7), formation of an absorption which resembles that of $MV^{\bullet+}$ can be observed (Figure 6). Since the rate constant of the reaction of OH radicals with MV^{2+} is more than an order of magnitude slower than with H_2S, the latter reaction predominates in these experiments. A complete spectrum, however, reveals that $MV^{\bullet+}$ is not the only radical produced by the reaction of $H_2S_2^{\bullet-}/HS^{\bullet}$ radicals with $MV^{\bullet 2+}$. Figure 7 shows the spectrum obtained at the end of the formation reaction observed in Figure 6. For comparison, the spectra of $H_2S_2^{\bullet-}$ and $MV^{\bullet+}$ are also shown in Figure 7. It is clear from the comparison of these spectra that, in addition to the spectral feature of $MV^{\bullet+}$, a new absorbing species is formed with λ_{max} = 485 nm. Assuming that the new species absorbs negligibly at the wavelength where $MV^{\bullet+}$ has its maximum absorption (λ_{max} = 394 nm, $\epsilon_{394} = 3.6 \times 10^4$ M^{-1} cm^{-1}), we can subtract the absorption of $MV^{\bullet+}$ and obtain the spectrum of the new absorbing species. This spectrum is also shown in Figure 7. We note that the spectrum of OH adducts to MV^{2+} has similar characteristics to the subtraction spectrum shown in Figure 7.[14] With the assumption mentioned above, we can calculate the fraction of total radical concentration that reacts to give $MV^{\bullet+}$ and from the latter estimate for the new species $\epsilon_{485} = 1.2 \times 10^4$ M^{-1} cm^{-1}. A plausible identification of this radical would be an $HS^{\bullet}$ or $S^{\bullet-}$ adduct to MV^{2+}. However, as shown below, this system is more complex than could be rationalized on the basis of only two radicals.

The subtracted spectrum in Figure 7 reveals little absorption at 600 nm. This substantiates the assumption that the absorption at the 390-nm region in the irradiated system containing 10^{-3} M of each H_2S and MV^{2+} is primarily due to MV^+ radicals. However, when the ratio of $[MV^{2+}]/[H_2S]$ is decreased, another radical (other than MV^+) which absorbs in the 600-nm region is also observed. The absorbances at three representative wavelengths (390, 490, and 600 nm) at various $[H_2S]$ and $[MV^{2+}]$ ratios are shown in Figure 8. As can be seen in Figure 8a, increasing $[H_2S]$ at constant (10^{-4} M) $[MV^{2+}]$ decreases the absorption at 490 nm and increases the yield observed at 390 nm. We therefore conclude that in the $HS^{\bullet}/H_2S_2^{\bullet-}$ equilibrated system, $HS^{\bullet}$ (or $S^{\bullet-}$) reacts with MV^{2+} to give an $HS^{\bullet}$ adduct (λ_{max} = 485 nm) while $H_2S_2^{\bullet-}$ reacts by electron transfer (eq 6 and 7).

$$(S^{\bullet-})HS^{\bullet} + MV^{2+} \rightarrow MV^{2+}HS^{\bullet} \quad (6)$$

$$H_2S_2^{\bullet-} + MV^{2+} \rightarrow MV^{\bullet+} + H_2S_2 \quad (7)$$

(14) Patterson, L. K.; Small, R. D.; Scaiano, J. C. *Radiat. Res.* **1977**, *72*, 218.

SCHEME I

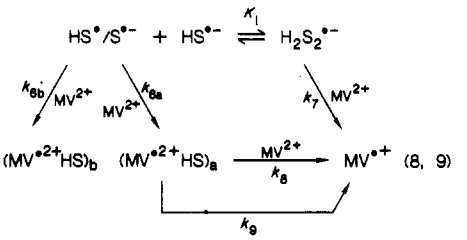

However, we also notice in Figure 8a that the absorbance at 600 nm increases only slightly upon increasing $[H_2S]$. This indicates the existence of a radical whose extinction coefficient at 600 nm is similar to that of $MV^{\bullet+}$, while its extinction at 390 nm is smaller than that of $MV^{\bullet+}$. On the other hand, we concluded from Figure 7 that such a radical does not exist at high $[MV^{2+}]$. Similar observations may be made in Figure 8b. The ratio of the absorption at 390 nm to that at 600 nm is clearly smaller at low $[MV^{2+}]$ and $[H_2S]$ than is the ratio for $MV^{\bullet+}$. At ~1 mM of both MV^{2+} and H_2S, the absorbances level off at the ratio expected for $MV^{\bullet+}$. It should be realized that the addition reaction 6 can yield in principle four different radicals, and we therefore propose that some of these addition products do absorb light at 600 nm. It was previously proposed that hydrogen atom addition to a carbon atom in the pyridinium ring of MV^{2+} produces a species that absorbs at 470 nm and negligibly so at 600 nm, while addition to the nitrogen atom yields a species of an absorption similar to that of $MV^{\bullet+}$.[15] The general features of the presently studied system are quite similar. Scheme I provides the simplest and most plausible explanation for our observations, including the kinetics to be described below. However, we like to point out that this scheme is not unique, and other more complex schemes might be invoked to rationalize our observations. Reaction 6a in this scheme is the addition reaction which produces the adduct absorbing at 600 nm, while reaction 6b produces the adduct which absorbs primarily at 485 nm. The change in the ratio of the absorptions at 390/600 nm with increasing $[MV^{2+}]$ (Figure 8b) necessitates reaction 8, i.e., conversion of the adduct to the $MV^{\bullet+}$ radical cation by its reaction with MV^{2+}. It should be noted here that the rate of the reaction of MV^{2+} with $HS^{\bullet}/H_2S_2^{\bullet-}$ is slow enough under the conditions used to allow establishment of equilibrium 1 during this reaction. On the other hand, at low MV^{2+} concentrations, some $HS^{\bullet}/H_2S_2^{\bullet-}$ radicals may escape scavenging by MV^{2+} due to reaction 2. A conversion reaction which is independent of $[MV^{2+}]$ (reaction 9) is indicated by the kinetic analysis.

In an attempt to verify Scheme I, several experiments were performed at pH's other than 7. At low pH's, the formation of $H_2S_2^{\bullet-}$ is suppressed since $[HS^-]$ is low enough to preclude reaction 1. In the pH range 2.0–4.0, no formation of any MV^+ radicals or the addition products could be observed (10^{-3} M H_2S, $(0.1-1.0) \times 10^{-3}$ M MV^{2+}, N_2O saturated). This observation indicates that $HS^{\bullet}$ is not the reactive radical in reaction 6. On the other hand, at high pH's, the yield of $H_2S_2^{\bullet-}$ and its lifetime are substantially reduced as compared to neutral solutions due to various deprotonation reactions.[4] When 10^{-3} M MV^{2+} is added to 10^{-3} M H_2S solution at pH 12, the three bands at 390, 485, and 600 nm are again observed following the irradiation. The relative absorbances, however, are quite different from those obtained at pH 7 under otherwise the same conditions. While the ratio of the 390- to 600-nm absorbance is similar to that in MV^+, the absorbance at 485 nm is nearly the same as the one at 390 nm. The effect of pH leads us to conclude the $S^{\bullet-}$ radicals are those participating in the addition reaction. From the relative absorbances, we calculated that, at pH 12, 70% of the total radicals produce the adduct which does not proceed to give $MV^{\bullet+}$ radicals.

Since, as mentioned at the beginning of this section, MV^{2+} probably forms ion pairs with HS^-, the question may arise as to

(15) Solar, S.; Solar, W.; Getoff, N.; Holcman, J.; Sehested, K. *J. Chem. Soc. Faraday Trans. 1* **1984**, *80*, 2929. Solar, S. *J. Phys. Chem.* **1984**, *88*, 5624.

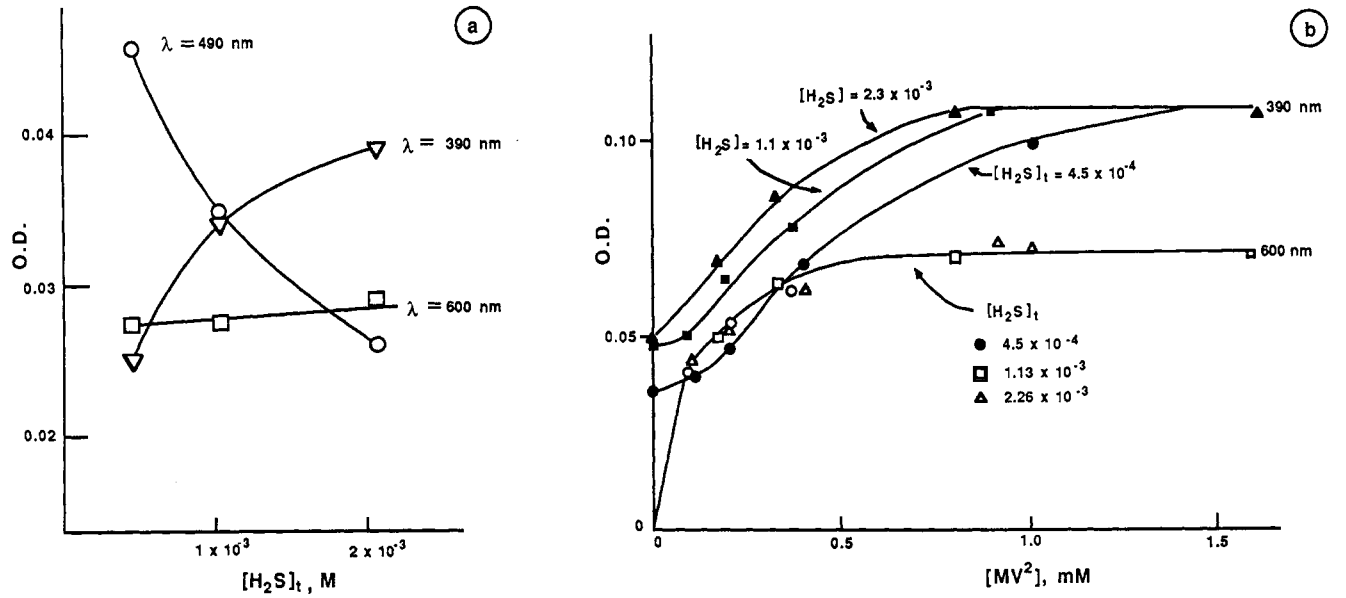

Figure 8. (a) Dependence of the absorbance at 390, 490, and 600 nm, at the end of the formation process, on $[H_2S]$. $[MV^{2+}] = 10^{-4}$ M. (b) Same absorbances as a function of $[MV^{2+}]$ at several H_2S concentrations. Solid symbols for 390 nm, open symbols for 600 nm: ○, $[H_2S] = 4.5 \times 10^{-4}$ M; □, $[H_2S] = 1.1 \times 10^{-3}$ M; △, $[H_2S] = 2.3 \times 10^{-3}$ M.

the effect of such ion pairing on the present results and their analysis. In particular, we were concerned that the reaction of $OH^\bullet$ radicals with an (MV^{2+}--HS^-) ion pair may produce radicals other than those discussed above (e.g., direct addition of OH). To check this point, we have studied the reaction of $HS^\bullet/H_2S_2^{\bullet-}$ with MV^{2+} where the former radicals were produced from $^\bullet CH_2C(CH_3)_2OH$ radicals in the presence of 1 M 2-methyl-2-propanol. Under these conditions and in N_2O-saturated solution, all the primary radicals are rapidly converted to the $^\bullet CH_2C(CH_3)_2OH$ radicals. The latter have been shown to produce $HS^\bullet/H_2S_2^{\bullet-}$ radicals[16] through the reaction

$$R^\bullet + H_2S \underset{}{\overset{k_{10}}{\rightleftharpoons}} R\dot{S}H_2 \rightarrow SH^\bullet + RH \qquad (10)$$

where RH is 2-methyl-2-propanol. The radicals obtained from 2-methyl-2-propanol have been shown to be unreactive toward MV^{2+}.[17] The absorption spectrum obtained under the same conditions as in Figure 7, except for the high 2-methyl-2-propanol concentration, is identical with the one shown in this figure (open squares), including the peaks at 394, 485, and 600 nm. We therefore conclude that in both experiments, regardless of the sources of $HS^\bullet/H_2S_2^{\bullet-}$ radicals, the same products are obtained.

The kinetics of the formation of radicals containing the viologen moiety in the presence of 1 M 2-methyl-2-propanol were found to be independent of wavelength. The rate of formation is also independent of $[MV^{2+}]$ but increases with $[H_2S]$. These observations are reflected in Figure 9. These results can be understood by assuming that the rate-determining step is the decomposition of the $R\dot{S}H_2$ radicals in reaction 10. With this assumption, the observed rate of formation of MV^{2+}-containing radicals (or $H_2S_2^{\bullet-}$ radicals when MV^{2+} is absent) is given by

$$\frac{1}{k_{obsd}} = \frac{1}{k_{10}} + \frac{1}{K_{10}k_{10}[H_2S]} \qquad (11)$$

The results of Figure 9 adhere to this expectation, leading to $k_{10} = 8.3 \times 10^4$ M^{-1} s^{-1} and $K_{10} = 1.4 \times 10^3$ M^{-1} in the presence of MV^{2+} and $k_{10} = 2.0 \times 10^5$ M^{-1} s^{-1} and $K_{10} = 0.85 \times 10^3$ M^{-1} in its absence. Karmann and Henglein obtain 1.3×10^5 M^{-1} s^{-1} and 1.0×10^3 M^{-1}, respectively, at pH 6.[16] The fact that the rates in the presence of MV^{2+} are slower than in its absence may indicate some modification of the kinetics and equilibrium due to ion pairing of HS^-. Nevertheless, the assumption that this ion pairing does not divert the reaction with OH radicals to different routes seems to hold.

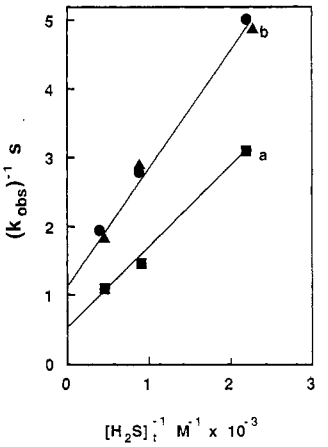

Figure 9. Dependence of the observed first-order rate constant for the formation of $H_2S_2^{\bullet-}$ radicals (a) and formation of MV^+/MV^+HS radicals (b) on $[H_2S]_t$ in the presence of 1 M 2-methyl-2-propanol at pH 7: (a) ■, no MV^{2+}, followed at λ = 380 nm. (b) ●, 0.1×10^{-3} M MV^{2+}; ▲, 2.0×10^{-3} M MV^{2+}, followed at 600 and 390 nm.

Kinetics of the formation of $MV^{\bullet+}$ and ($MV^{2+}HS$) radicals in the absence of alcohol according to Scheme I was studied only briefly at the three selected wavelengths. With the assumption mentioned above, i.e., that the product of reaction 6a has an extinction coefficient at 600 nm similar to that of $MV^{\bullet+}$, it is easy to see that, when reactions 8 and 9 are complete

$$\frac{A_{600}}{A_{490}} = \frac{k_{6a}}{k_{6b}} + \frac{k_7}{k_{6b}}K_1[HS^-]$$

The results of Figure 8a follow this relationship to yield $k_{6a}/k_{6b} = 0.5$ and $k_7/k_{6b} = 4.6 \times 10^{-2}$. Thus, ~70% of the addition products ($k_{6b}/k_6 = 0.67$) do not proceed to give $MV^{\bullet+}$ and the rate of direct electron transfer from $H_2S_2^{\bullet-}$ is ~30 times slower than the addition reactions ($k_6/k_7 = 31$). The observed rate of formation of the absorptions at 600 nm is linear with $[MV^{2+}]$, $(0.1-1) \times 10^{-3}$ M, leading to an observed rate constant $k_{obsd} = 3.5 \times 10^8$ M^{-1} s^{-1}. Since the same rate constant is obtained from the formation of absorption at 390 nm and since it is nearly independent of $[H_2S]$, we believe that this rate constant is equal to $k_{6a} + k_7$ and that k_8 is larger than this rate constant. The linear dependence of the rate on $[MV^{2+}]$, however, yields a nonzero intercept of $k = 7 \times 10^4$ s^{-1}. This may be identified in Scheme

(16) Karmann, W.; Henglein, A. *Ber. Bunsenges. Phys. Chem.* **1967**, *71*, 421.
(17) Venturi, M.; Mulazzani, Q. G.; Hoffman, M. Z. *Radiat. Phys. Chem.* **1984**, *23*, 229.

I as k_9. The observed rate of the formation of the radicals when followed at 490 nm is ca. 50% faster than at 600 nm. However, since at this wavelength the formation and disappearance through reactions 8 and 9 overlap, this may introduce such an artifact.

Neither $MV^{\bullet+}$ nor the addition product is found to be stable for more than a few milliseconds when formed through Scheme I. This was found to be the case in the pH range of 7-12 at any of the wavelengths studied. The absorption at 490 nm in this pH range decays faster than the 600-nm absorption ($\tau_{1/2}$ = 80 μs). Both exhibit a mixture of first- and second-order rate law. The faster decay at 490 nm is attributed to partial conversion of the adduct $MV^{2+}SH^{\bullet}$ to MV^{+} overlapping with the radical-radical recombination reaction 12.

$$2MV^{2+}SH^{\bullet} \rightarrow P \quad (12a)$$

$$MV^{2+}SH^{\bullet} + MV^{\bullet+} \rightarrow P \quad (12b)$$

Conclusions

The main observations of this study may be summarized as follows: (a) sulfide radicals $HS^{\bullet}/HS^{\bullet-}$ as well as $H_2S_2^{\bullet-}$ react with oxygen to produce eventually $O_2^{\bullet-}$ radicals; (b) photolysis of $H_2S_2^{\bullet-}$, the only species of the sulfide radicals that absorbs light in the near-UV region, leads to dissociation to its components $HS^{\bullet}$ and HS^{-}; (c) the reaction of $HS^{\bullet}/H_2S_2^{\bullet-}$ with MV^{2+} produces $MV^{\bullet+}$ radicals, as well as some addition product radicals, which strongly absorb light in the region of 490 nm.

While all the reactions studied here were performed in homogeneous solutions, some implications for photochemical reactions of colloidal sulfides may be indicated. As previously suggested, $S^{\bullet-}$ radicals efficiently react with oxygen. This is perhaps not surprising, since the standard reduction potential of the O_2/HO_2 couple (-0.03 V vs. NHE at pH 0) is much more positive than that of the $S/SH^{\bullet}$ couple. The latter could be estimated to be ~-1.3 V from the calculated E°_{HS/HS^-} = 1.4 V,[2b] the two-electron standard redox potential E°_{S/HS^-} = -0.07 V, and the latent heat of sublimation of sulfur (0.15 V). The dimeric radical $H_2S_2^{-}$ should still be a strong reductant since the equilibrium constant for reaction 1 provides only 0.24 V to its stabilization. The fact that we observe primarily addition reactions for $S^{\bullet-}$ radicals in spite of the large driving force for reduction probably is due to large solvent reorganization in the electron-transfer reaction. Furthermore, the superoxide radical obtained in this reaction may continue to react with the colloidal sulfide or with H_2S ($E^{\circ}_{HO_2/H_2O_2}$ = 1.42 V at pH 0). While this reaction does not occur on CdS colloids,[18] we have recently found that $O_2^{\bullet-}$ does corrode As_2S_3 colloids.[19] Such a reaction is, in fact, hole injection to the valence band of the colloid and will result in the phenomenon of "current doubling".[20]

The reaction of sulfide radicals with MV^{2+} is rather important, since MV^{2+} is often used as an electron acceptor in photoexcitation of sulfide colloids. Our results indicate that sulfide radicals, certainly in the bulk of the solution and probably at the colloid surface, may produce the $MV^{\bullet+}$ radicals. This means, therefore, that, in addition to electron scavenging, $MV^{\bullet+}$ radicals may be produced by hole scavenging as well. Indeed, Rossetti and Brus[22] proposed two mechanisms for the production of $MV^{\bullet+}$ in excited CdS. The redox potentials are clearly in favor of such a reaction. Furthermore, as shown in this study, sulfide radicals also produce addition products upon their reaction with MV^{2+}. These are strongly absorbing in the green region of the spectrum. In the photolysis of CdS colloids in the presence of MV^{2+}, absorption in that region is often observed.[21] These have been attributed to $MV^{\bullet+}$ dimers. Our observations raise the possibility that an alternative species, the addition product, may also be present. It should be noted that, in the absence of electron donors, scavenging of electrons following excitation of CdS leads to destruction of the colloid. This has been shown to result in strong bleaching of the CdS absorption at 490 nm.[23] Reaction of $S^{\bullet-}/HS^{\bullet}$ with MV^{2+} to give the adduct radical in the photolysis experiments is therefore difficult to observe in this region. On the other hand, when sulfide is used as a hole scavenger, higher yields of MV^{+} radicals are expected, due to efficient interception of the hole-electron recombination process, as well as reaction of the $HS^{\bullet}/S^{\bullet-}$ system with MV^{2+}.

Acknowledgment. The dedicated operation of the ANL Linac facility by D. Ficht and G. Cox is gratefully appreciated. This work was performed under the auspices of the Office of Basic Energy Sciences, Division of Chemical Science, U.S. DOE, under Contract No. W-31-109-ENG-38.

Registry No. MV^{2+}, 4685-14-7; $MV^{\bullet+}$, 25239-55-8; $HS^{\bullet}$, 13940-21-1; HS^{-}, 15035-72-0; $H_2S_2^{\bullet-}$, 12293-10-6; H_2S, 7783-06-4; O_2, 7782-44-7.

(18) Henglein, A. *J. Phys. Chem.* **1982**, *86*, 2293.
(19) Mills, G.; Meisel, D., to be submitted for publication.
(20) Morrison, R. S. *Electrochemistry at Semiconductor and Oxidized Metal Electrodes*; Plenum: New York, 1980; p 209.
(21) (a) Serpone, N.; Sharma, D. K.; Jamieson, M. A.; Grätzel, M.; Ramsden, J. J. *Chem. Phys. Lett.* **1985**, *115*, 473. (b) Kuczynski, J.; Thomas, J. K. *J. Phys. Chem.* **1983**, *87*, 5498.
(22) Rossetti, R.; Brus, L. E. *J. Phys. Chem.* **1986**, *90*, 558.
(23) Albery, W. I.; Brown, G. T.; Darwent, J. R.; Saievar-Iranizad, E. *J. Chem. Soc., Faraday Trans. 1* **1985**, *81*, 1999.

A Potential Energy Function for the Hydroperoxyl Radical

William J. Lemon† and William L. Hase*

Department of Chemistry, Wayne State University, Detroit, Michigan 48202 *(Received: August 8, 1986; In Final Form: October 27, 1986)*

A switching function formalism is used to derive an analytic potential energy surface for the $O + OH \rightleftharpoons HO_2 \rightleftharpoons H + O_2$ reactive system. Both experimental and ab initio data are used to derive parameters for the potential energy surface. Trajectory calculations for highly excited HO_2 are performed on this surface. From these trajectories quasi-periodic eigentrajectories are found for vibrational levels near the HO_2 dissociation threshold with small amounts of quanta in the OH stretch mode and large amounts of quanta in the OO stretch mode.

I. Introduction

The hydroperoxyl radical is an important transient intermediate in a variety of reaction systems in photochemistry,[1] atmospheric chemistry,[2,3] oxidation and combustion processes,[4] and biological chemistry.[5] The reaction

$$H + O_2 \rightarrow HO_2^* \rightarrow O + OH$$

is the single most important chemical reaction in combustion.[6] It initiates the chain branching ignition phenomenon in the ox-

† Undergraduate research fellow.

(1) Paukert, T. T.; Johnston, H. S. *J. Chem. Rev.* **1972**, *56*, 2824.
(2) Rowland, F. S.; Molina, M. *Rev. Geophys. Space Phys.* **1975**, *13*, 1.

0022-3654/87/2091-1596$01.50/0